British Journal of Pharmacology (1998) 123, 1385–1394

Evidence for the existence of [^{3}H]-trimetazidine binding sites involved in the regulation of the mitochondrial permeability transition pore

[1,2,5]Didier Morin, [1]Aziz Elimadi, [1]Rosa Sapena, [3]Aimé Crevat, [4]Pierre-Alain Carrupt, [4]Bernard Testa & [1]Jean-Paul Tillement

[1]Département de Pharmacologie, [2]CNRS and [1]IM3, Faculté de Médecine de Paris XII, Créteil, France, [3]Laboratoire de Biophysique, Faculté de Pharmacie, Marseille, France and [4]Institut de Chimie Thérapeutique, Université de Lausanne, CH-1015 Lausanne, Switzerland

1 Trimetazidine is an anti-ischaemic drug effective in different experimental models but its mechanism of action is not fully understood. Data indicate that mitochondria could be the main target of this drug. The aim of this work was to investigate the binding of [^{3}H]-trimetazidine on a purified preparation of rat liver mitochondria.

2 [^{3}H]-trimetazidine binds to two populations of mitochondrial binding sites with K_d values of 0.96 and 84 μM. The total concentration of binding sites is 113 pmol mg^{-1} protein. Trimetazidine binding sites are differently distributed. The high-affinity ones are located on the outer membranes and represent only a small part (4%) of total binding sites, whereas the low-affinity ones are located on the inner membranes and are more abundant (96%) with a $B_{max} = 108$ pmol mg^{-1} protein.

3 Drug displacement studies with pharmacological markers for different mitochondrial targets showed that [^{3}H]-trimetazidine binding sites are different from previously described mitochondrial sites.

4 The possible involvement of [^{3}H]-trimetazidine binding sites in the regulation of the mitochondrial permeability transition pore (MTP), a voltage-dependent channel sensitive to cyclosporin A, was investigated with mitochondrial swelling experiments. Trimetazidine inhibited the mitochondrial swelling induced by Ca^{2+} plus *tert*-butylhydroperoxide (*t*-BH). This effect was concentration-dependent with an IC_{50} value of 200 μM.

5 Assuming that trimetazidine effectiveness may be related to its structure as an amphiphilic cation, we compared it with other compounds exhibiting the same chemical characteristic both for their ability to inhibit MTP opening and to displace [^{3}H]-trimetazidine bound to mitochondria. Selected compounds were drugs known to interact with various biological membranes.

6 A strong correlation between swelling inhibition potency and low-affinity [^{3}H]-trimetazidine binding sites was observed: $r = 0.907$ ($n = 24$; $P < 0.001$).

7 These data suggest that mitochondrial sites labelled with [^{3}H]-trimetazidine may be involved in the MTP inhibiton.

Keywords: Trimetazidine; specific binding sites; rat liver mitochondria; mitochondrial permeability transition pore (MTP); mitochondrial swelling

Introduction

Trimetazidine, 1-(2,3,4-trimethoxybenzyl)piperazine (Figure 1) is an anti-ischaemic drug effective in different experimental models including cultured cells, isolated organs or animal models of ischaemia (Harpey *et al*., 1989). Its mechanism of action is not fully understood but data indicate that it affects both metabolic functions and ion permeabilities in mitochondria. Indeed Lavanchy *et al*. (1987) showed that trimetazidine preserved adenosine 5′-triphosphate (ATP) and phosphocreatine levels in myocardial fibres after experimental ischaemia. Guarnieri & Muscari (1993) demonstrated that trimetazidine improved mitochondrial functions during ischaemic damage while Salducci *et al*. (1996) showed that trimetazidine restored the ATP synthesis in isolated mitochondria previously exposed to a Ca^{2+} overload either alone or associated with cyclosporin A. More recently, it was also observed that trimetazidine counteracted the mitochondrial permeability transition induced by Ca^{2+} overload associated with the prooxidant *tert*-butylhydroperoxide (*t*-BH) and that this effect was independent of that induced by cyclosporin A in both its kinetics and mechanism of action (Elimadi *et al*., 1997). The biochemical events mediating this transition are not fully understood but probably involve the formation of a giant pore, called the mitochondrial permeability transition pore (MTP; Haworth and Hunter, 1979), allowing the exchange of small solutes (<1500 Da) across the inner membrane (Zoratti & Szabo', 1995). It is thus clear that trimetazidine acts on mitochondrial function in at least two different ways, as a mitochondrial Ca^{2+} releaser when the giant pore is closed, and by inducing its closure when it is open.

These results led us to look for specific trimetazidine binding sites in mitochondria. In the present study, radio-labelled trimetazidine was used to demonstrate the existence of two different classes of specific trimetazidine binding sites. These sites are located on both the inner and outer membranes of purified liver mitochondria and appear to be distinct from other mitochondrial sites described so far. To study the functional significance of trimetazidine binding sites, we hypothesized that, as trimetazidine is an amphiphilic cation (organic cation with a large hydrophobic moiety) and as such able to bind to membranes, this physico-chemical characteristic was possibly

[5]Author for correspondence at: Département de Pharmacologie, Faculté de Médecine de Paris XII, 8 rue du Général Sarrail, F-94010, Créteil, France.

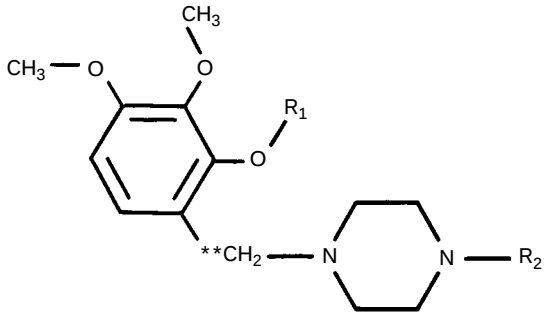

	R_1	R_2
Trimetazidine	CH_3*	H
S-00226	CH_3	C_2H_5
S-00240	CH_3	$CH(C_6H_5)_2$
S-17316	H	CH_3
S-64329	CH_3	CH_2-C_6H_5

Figure 1 Chemical structures of trimetazidine (1-(2,3,4-trimethoxybenzyl)piperazine) and trimetazidine derivatives, and labelling positions. *Tritium; **carbon 14.

related to its MTP closing potency. Thus, we compared trimetazidine with other amphiphilic cations for their ability to displace [^{3}H]-trimetazidine binding and to inhibit Ca^{2+} plus *t*-BH induced swelling, an indicator of MTP occurrence.

Methods

Subcellular fractionation of liver

Male Wistar rats (200–220 g) were decapitated. The liver was removed, weighed and cut in small pieces in ice-cold buffer A (50 mM Tris, 250 mM sucrose, 5 mM EGTA, pH = 7.8 at 4°C). The pieces were rinsed five times and homogenized in the same buffer (10 g tissue/60 ml buffer A) in a dounce glass homogenizer (ten slow up and down strokes by hand). The homogenate was filtered through a nylon mesh and centrifuged for 10 min at 600 *g* at 4°C. The resulting pellet was washed twice in buffer A, once in buffer B (50 mM Tris, 250 mM sucrose, pH = 7.8 at 4°C) and sedimented at 600 *g*. The final washed pellet, termed the 'nuclear fraction', was kept in buffer B. The supernatant was centrifuged for 10 min at 3300 *g* and the same rinsing procedure was applied to the resulting pellet. The new resulting pellet was kept in buffer B and was termed the 'heavy mitochondrial fraction (M_H)'. The supernant (from 10 min at 3300 *g*) was then centrifuged at 15,000 *g* for 10 min: the resulting pellet was washed as described above, kept in the buffer B and termed the 'light mitochondrial fraction (M_L)'. The resulting supernatant was centrifuged at 170,000 *g* for 1 h (Sorvall A 841 rotor) to obtain a pellet corresponding to the 'microsomal fraction'. This pellet was also resuspended in buffer B.

The four subcellular fractions and a sample of the initial homogenate were used immediately (binding assays) or stored at −20°C (enzyme assays).

All animal procedures used in this study were in strict accordance with the French Agency's policies on animal experimentation.

Purification of mitochondrial fractions

Mitochondria were purified by use of a method adapted from Koenig (1974). The fractions M_H and M_L (6 ml) were layered on a discontinuous density gradient of 5 ml each of 0.9, 1.2 and 1.4 M sucrose. The tubes were centrifuged at 63 500 *g* for 120 min (Beckman AH 627 rotor).

The M_H fraction was separated into three new fractions designated as M_{H_1} (0.9–1.2 M interface), M_{H_2} (1.2–1.4 M) and M_{H_3} (remaining pellet) fractions. The M_L fraction was also separated into three fractions designated as ML_{L_1} (0.9–1.2 M), M_{L_2} (1.2–1.4 M) and M_{L_3} (remaining pellet) fractions. The bands were recovered with a Pasteur pipette, each fraction was diluted in buffer B and centrifuged at 50 000 *g* for 10 min. The supernatants were discarded and the pellets suspended in buffer B. The different fractions were used immediately (binding assays) or stored at −20°C (enzyme assays).

The submitochondrial localization of [^{3}H]-trimetazidine binding sites was determined either in the M_{L_3} fraction by use of a digitonin solubilization method to separate the outer from the inner mitochondrial membrane as described by Anholt *et al*. (1986), or by osmotic shock and sonication exactly as described by Graham (1993a).

For swelling experiments mitochondria were prepared according to the method of Johnson & Lardy (1976) slightly modified by Salducci *et al*. (1996).

Enzyme assays

All enzymatic activities were determined by spectrophotometric methods by use of an Hitachi UV-3000 spectrophotometer and were shown to be linear in the tissue and protein concentration range used. Catalase (EC 1.11.1.6), succinate dehydrogenase (EC 1.3.99.1) and rotenone-insensitive NADPH cytochrome C reductase (EC 1.6.2.5) were assayed at room temperature as described by Graham (1993b).

The determination of monoamine oxidase (MAO; EC 1.4.3.4) activity was performed according to the method of Bembenek *et al*. (1990), with kynuramine as a substrate and monitoring the formation of 4-hydroxyquinoline at 316 nm. Cytochrome C oxidase (EC 1.9.3.1) activity was assayed at 37°C according to the method of Rustin *et al*. (1994) by monitoring the oxidation of ferrocytochrome C (prepared from type III horse heart cytochrome C (Sigma)) at 550 nm. Acid phosphatase (EC 3.1.3.2) was determined by means of a commercial kit (Sigma).

Binding experiments

Binding of [^{3}H]-trimetazidine was assayed as follows: 300 μl of the subcellular fractions (1.5–2 mg ml^{-1} protein) were incubated with 7–10 nM [^{3}H]-trimetazidine (83 Ci $mmol^{-1}$) and 24 to 28 different concentrations of competing drug or buffer B for 45 min at 25°C in a total volume of 400 μl. Specific binding was defined as the difference between total binding and binding in the presence of 1 mM trimetazidine or of the trimetazidine derivative, S-00226 (Figure 1) and was linear up to 3 mg ml^{-1} protein. For saturation analysis [^{14}C]-trimetazidine (0.5–300 μM; specific activity 54.9 mCi $mmol^{-1}$) was used and the non-specific binding was defined in the presence of 50 mM S-00226.

The kinetic association experiments were carried out for 60 min with a [^{3}H]-trimetazidine concentration of 8 nM. The reversibility of [^{3}H]-trimetazidine binding was demonstrated after a previous incubation of 45 min by dilution of the mitochondrial suspension (1/80) with incubation buffer B. These kinetic dissociation experiments were performed with a higher concentration (40 nM) of [^{3}H]-trimetazidine. In some kinetic experiments, binding of [^{3}H]-trimetazidine was studied in the presence of 6 μM S-00226. This concentration

was shown to inhibit specifically [3H]-trimetazidine binding to high-affinity sites without affecting its binding to low-affinity sites in inhibition experiments. This approach allowed us to ascribe an association rate constant to one of the dissociation rate constants and thus to estimate dissociation constants (K_d) from these kinetic values (see data analysis).

For [3H]-flunitrazepam binding studies, [3H]-flunitrazepam (7–8 nM) and purified mitochondria (M_{H_3}) (0.2 mg ml^{-1}) were incubated in a total volume of 500 μl at 25°C for 30 min. Non specific-binding was determined in the presence of 10 μM diazepam.

Binding experiments with [3H]-CGP-12177 (1.5 nM) were performed as previously described (Morin *et al*., 1992) with 100 μM isoprenaline to define non-specific binding.

Binding experiments with [3H]-nitrendipine, [3H]-idazoxan and [3H]-PK-11195 were performed as described by Zernig *et al*. (1990), Tesson *et al*. (1991) and Lefur *et al*. (1983), respectively.

At the end of each incubation, bound and free ligands were separated by rapid filtration through Whatman GF/B glass fibre filters (presoaked in 0.1% polyethylenimine). Each filter was washed twice with an additional 5 ml of ice-cold Tris-buffer (50 mM) and counted in a liquid scintillation counter Packard 1600 TR with an efficiency of 45%. The filtration process was rapid enough to avoid the dissociation of radiolabelled trimetazidine from its binding sites. In addition, in all cases radiolabelled trimetazidine binding to glass fibre filters was very low, less than 0.05% of total ligand concentration. Protein concentrations were determined according to the method of Lowry *et al*. (1951) with bovine serum albumin as a standard.

Mitochondrial swelling

Mitochondrial volume was assessed by measuring the change in absorbance at 520 nm by using an Hitachi UV-3000 spectrophotometer. The method of Halestrap & Davidson (1990) was used with some modifications. Experiments were carried out at 25°C in a Tris buffer consisting of 150 mM sucrose, 5 mM Tris, 0.5 μg of rotenone ml^{-1} and 0.5 μg of antimycin ml^{-1}, pH 7.4. In a total volume of 1.8 ml, mitochondria (2 mg) were preincubated for 10 min before the addition of 100 μM $CaCl_2$. Swelling was initiated 4 min later by the addition of 10 μM *t*-BH.

Materials

Labelled (^3H and ^{14}C) and unlabelled trimetazidine and trimetazidine derivatives (Figure 1) were kindly provided by Servier Laboratories (Neuilly-sur-Seine, France). [3H]-nitrendipine (75.3 Ci $mmol^{-1}$), [3H]-flunitrazepam (85.8 Ci $mmol^{-1}$), [3H]-PK-11195 (1-(2-chlorophenyl)-N-methyl-N-(1-methylpropyl)-3-isoquinoline carboxamide; 86.4 Ci $mmol^{-1}$), [3H]-idazoxan (60 Ci $mmol^{-1}$) and [3H]-CGP-12177 ((−)4-(3-*t*-butylamino - 2 - hydroxypropoxy)benzimidazol - 2 -one; 57.2 Ci-$mmol^{-1}$) were from New England Nuclear (Les Ulis, France). Other chemicals were obtained from Sigma (St Quentin Fallavier, France), Merck (Nogent-sur-Marne, France) or Research Biomedical International/Bioblock Scientific (Illkirch, France) and were of the highest purity available.

Data analysis

According to the law of mass action, bound and free ligand concentrations are related as follows:

$$B = \frac{B_{max_H} F}{F + K_{d_H}} + \frac{B_{max_L} F}{F + K_{d_L}} \quad (1)$$

The binding data for equilibrium saturation experiments were fitted to this equation describing the interaction of a selective ligand with two classes of high (H) and low (L) affinity binding sites. B_{max} and K_d denote the site density and the dissociation constant of each class, respectively.

In kinetic studies, binding data for dissociation kinetic experiments were fitted either to Equation (2) or to Equation (3) assuming the presence of one class or two classes of binding sites, respectively:

$$B = B_{eq}.e^{-k_{-1}.t} \quad (2)$$

$$B = B_{eq_A}.e^{-k_{1A}.t} + B_{eq_B}.e^{-k_{1B}.t} \quad (3)$$

Beq and k_{-1} represent the bound ligand at equilibrium and the dissociation rate constant, respectively. For each experiment, the one-site and the two-site models were compared and the best fit was chosen according to the Aikake criterion.

The same protocol was applied to association kinetic experiments, the data being fitted to the following equations:

$$\text{one} - \text{site model} : B = B_{eq}\ (1 - 1/e^{k_{obs}.t}) \quad (4)$$

$$\text{two} - \text{site model} : B = B_{eq_A}\ (1 - 1/e^{k_{obsA}t}) + B_{eq_B}\ (1 - 1/e^{k_{obsB}t}) \quad (5)$$

where $k_{obs} = k_{+1}$. Lt . B_{max}/B_{eq} and k_{+1} and Lt represent the association rate constant and the total ligand concentration, respectively. This equation allows the determination of an association rate constant for each class of binding sites (k_{+1A} and k_{+1B}) and then the calculation of a kinetic dissociation constant: $K_d = k_{-1}/k_{+1}$ for each process (K_{d_H} and K_{d_L}).

In inhibition experiments, the displacement curves were fitted to the general binding isotherm (Hill model):

$$B = \frac{B_{eq}.IC_{50}^{n_H}}{IC_{50}^{n_h} + C^{n_H}} \quad (6)$$

where B is the number of binding sites observed in the presence of a particular inhibitor concentration (C), B_{eq} the bound ligand at equilibrium, IC_{50} the concentration that inhibits 50% of the maximal binding and n_H the pseudo-Hill coefficient (Weiland & Molinoff, 1981). A n_H value equal to 1 corresponds to a competitive interaction and thus indicates the presence of one class of binding sites. When the n_H value was statistically lower than 1 (according to the Aikake criterion), a competitive model considering a competitive interaction including two classes of binding sites was applied. The following equation was used:

$$B = \frac{B_{eq_H}.IC_{50H}}{IC_{50H} + C} + \frac{B_{eq_L}.IC_{50L}}{IC_{50L} + C} \quad (7)$$

Data from all binding experiments were analysed by means of non-linear regression with commercially available software (Microparm, INSERM 1990; Urien, 1995). All data are presented as the mean ± s.e. of three or more individual experiments. The initial rate of swelling was expressed as $\Delta abs/\Delta t$ mg^{-1} protein.

Results

Subcellular localization of [3H]-trimetazidine binding sites

[3H]-trimetazidine binding, along with the activities of representative markers, i.e. cytochrome C oxidase (mitochon-

dria), NADPH cytochrome C reductase insensitive to rotenone (microsomes), catalase (peroxisomes), acid phosphatase (lysosomes) and [3H]-CGP-12177 binding (plasma membranes), were studied on different subfractions from the liver. Table 1 shows that [3H]-trimetazidine was bound to mitochondrial fractions ($M_H + M_L$) but that substantial binding was also present in microsomal and nuclear fractions. Inhibition experiments revealed that trimetazidine binding was competitive on the microsomal fraction (pseudo-Hill coefficient $n_H \sim 1$) but not on the three other fractions ($n_H < 1$; Table 1), IC_{50} values of all fractions being in the same range. Since a large percentage of [3H]-trimetazidine binding was found in the non-mitochondrial fractions, it appeared necessary to evaluate the contamination of mitochondrial preparations by other organelles. This was done by checking the distribution of compartmental markers as shown in Figure 2.

Table 1 [3H]-trimetazidine binding to subcellular fractions of rat hepatocytes

Fractions	IC_{50} (μM)	*Bound* (fmol mg^{-1})	n_H
Nucleus	3.40±0.98	35.3±6.0	*0.73±0.14
Microsomes	2.00±0.30	100.7±14.4	0.85±0.10
Light mitochondria	3.50±0.40	76.7±22.1	*0.77±0.06
Heavy mitochondria	4.90±0.50	43.3±12.6	*0.70±0.04

Protein (2 mg ml^{-1}) from nucleus, microsomes, light mitochondria or heavy mitochondria were incubated with 8 nM [3H]-trimetazidine for 45 min at 25°C. Non-specific binding was defined in the presence of 1 mM S-00226 and represented 24% of the binding in nucleus, 17% in the light mitochondria, 24% in the heavy mitochondria and 11% in the microsomal fraction. n_H is the pseudo-Hill coefficient. Each value is the mean±s.e. of three to four separate experiments. *Statistically less than 1.

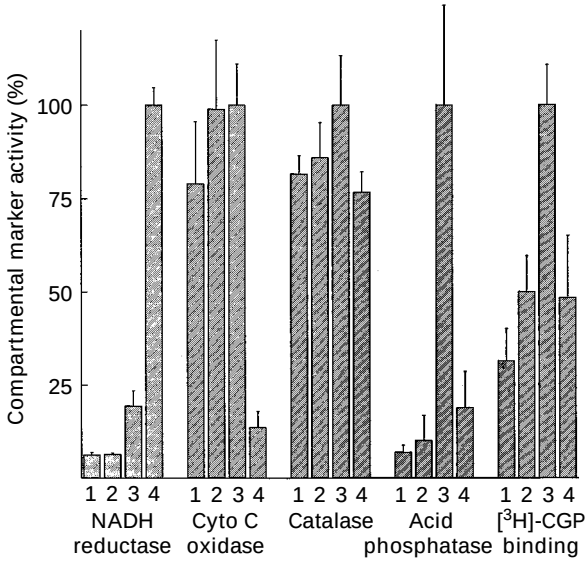

Figure 2 Distribution of compartmental markers in subcellular fractions obtained from rat liver homogenates. For each marker, the activity of a particular fraction was expressed as a percentage of the highest activity (100%) obtained for one of the fractions. The maximal activities of the different markers were 3.14 nmol min^{-1} mg^{-1} protein for NADPH-cytochrome C reductase, 5.62 nmol min^{-1} mg^{-1} protein for cytochrome (cyto) C oxidase, 0.53 μmol min^{-1} mg^{-1} protein for acid phosphatase, 5.87 nmol min^{-1} mg^{-1} protein for catalase and 9.37 fmol mg^{-1} protein for the binding of [3H]-CGP-12177. (1) Nucleus; (2) heavy mitochondria; (3) light mitochondria; (4) microsomes.

Among the mitochondrial fractions, the light fraction, M_L, was the most contaminated with peroxisomes, lysosomes and plasma membranes, as attested by the specific activity of their representative markers. The heavy fraction, M_H, was devoid of lysosomes and microsomes and its major contaminants were peroxisomes and to a lesser extent plasma membranes. The large binding recovery in the nuclear fraction can be attributed to the presence of mitochondria, as assessed by cytochrome C oxidase activity remaining in this fraction. However, this cellular distribution study reveals that [3H]-TMZ binding sites cannot be strictly associated with the mitochondrial compartment since on the one hand [3H]-TMZ binding seems ubiquitous and on the other hand mitochondrial fractions are lightly contaminated by other organelles. Therefore a purification of mitochondrial fractions was considered necessary.

To this end, M_H and M_L fractions were layered on a discontinuous density gradient of sucrose and centrifuged as detailed in the experimental section. [3H]-trimetazidine binding and specific activities of compartmental markers were then tested on each fraction obtained before and after centrifugation. The sucrose gradient allowed us to separate a mitochondrial fraction (M_{H_3}) with a very high cytochrome C oxidase activity and practically no microsomes and plasma membranes (Figure 3). The only contamination remaining in this fraction was due to the presence of peroxisomes and to a lesser extent of lysosomes. However, no correlation was observed between [3H]-trimetazidine binding and the lysosomal or peroxisomal marker enzymes (Elimadi & Morin, unpublished observations). The M_{H_3} fraction was therefore considered as a purified mitochondrial fraction and was used in subsequent experiments.

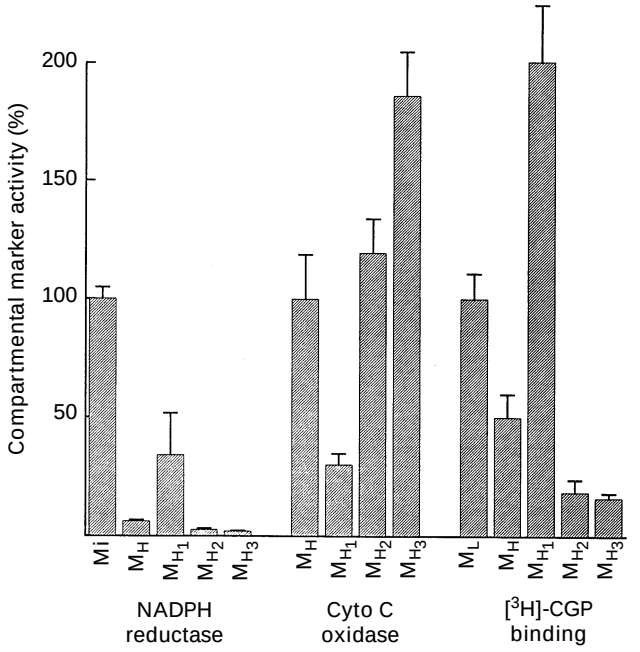

Figure 3 Distribution of compartmental heavy markers in heavy mitochondrial fraction before (M_H) and after (M_{H_1}, M_{H_2}, M_{H_3}) separation on discontinuous sucrose gradient. For each marker, the activity of a particular fraction was expressed as a percentage of the highest activity (100%) obtained for one of the fractions. The maximal activities of the different markers were 5.62 nmol min^{-1} mg^{-1} protein for cytochrome C oxidase, 3.14 nmol min^{-1} mg^{-1} protein for NADPH-cytochrome C reductase and 9.37 fmol mg^{-1} protein for the binding of [3H]-CGP-12177. M_L: light mitochondria; Mi: microsomes.

Characterization of [3H]-trimetazidine binding sites on purified mitochondria (M_{H_3} fraction)

Specific [3H]-trimetazidine binding to mitochondria reached equilibrium after 40 min incubation at 25°C. The association curve was biphasic and involved both fast and slow processes showing the presence of two families of binding sites (Figure 4a). k_{obs} values, determined by means of Equation (5), were $k_{obsA} = 1.99 \pm 0.47$ and $k_{obsB} = 0.065 \pm 0.011$ corresponding to calculated association rate constants of $k_{+1A} = 1.46 \pm 0.34 \times 10^4$ M^{-1} min^{-1} and $k_{+1B} = 2.08 \pm 0.35 \times 10^4$ M^{-1} min^{-1}. Dilution of the suspension (1/80) induced a biphasic dissociation of the ligand from its binding sites (Figure 4b). The calculated dissociation rate constants were $k_{-1A} = 1.81 \pm 0.31$ min^{-1} ($t_{\frac{1}{2}} = 23$ s) and $k_{-1B} = 0.077 \pm 0.031$ min^{-1} ($t_{\frac{1}{2}} = 9$ min).

The same kinetic studies were performed in the presence of 6 μM S-00226 (Figure 1), a concentration that inhibits specifically [3H]-trimetazidine binding to the high-affinity sites (see below, Figure 6). The kinetic association curve became monophasic and the slow process was eliminated (Figure 4a). In the same way S-00226 did not modify the fast kinetic dissociation binding process but strongly reduced (by 50%) the binding of trimetazidine associated with the slow binding process (Figure 4b). The latter was not completely suppressed but the experiments demonstrated that the fast association and dissociation processes (k_{+1A} and k_{-1A}) corresponded to [3H]-trimetazidine binding to the low-affinity binding sites. From these experiments the kinetic dissociation constants of [3H]-trimetazidine for each class of binding sites could be calculated: $K_{d_L} = k_{-1A}/k_{+1A} = 124$ μM and $K_{d_H} = k_{-1B}/k_{+1B} = 3.7$ μM. These values were comparable to the IC_{50} and K_d values determined in displacement and equilibrium experiments, respectively (see below).

Given that the affinity of trimetazidine for mitochondria was relatively low, equilibrium binding experiments were performed with [14C]-trimetazidine. These experiments confirmed the presence of two populations of trimetazidine

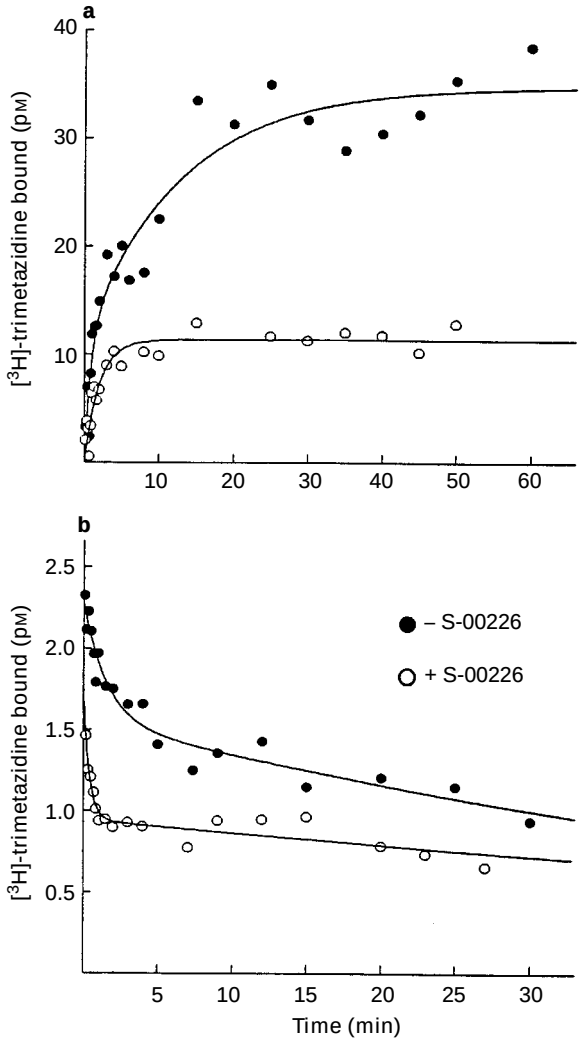

Figure 4 Association (a) and dissociation (b) kinetics of [3H]-trimetazidine to rat liver mitochondria. [3H]-trimetazidine (8 nM for association, 40 nM for dissociation) and mitochondria (2 mg ml^{-1}) were incubated in presence or absence of 6 μM of S-00226. The kinetic parameters were determined by a non-linear regression analysis by use of a one- or a two-site model. In this particular experiment low-affinity binding sites (fast processes) represented about 33% of the total sites. Non-specific binding was defined in the presence of 1 mM trimetazidine and corresponded to 31% of the total binding at equilibrium. For example specific binding amounted to 3207 d.p.m. in (a).

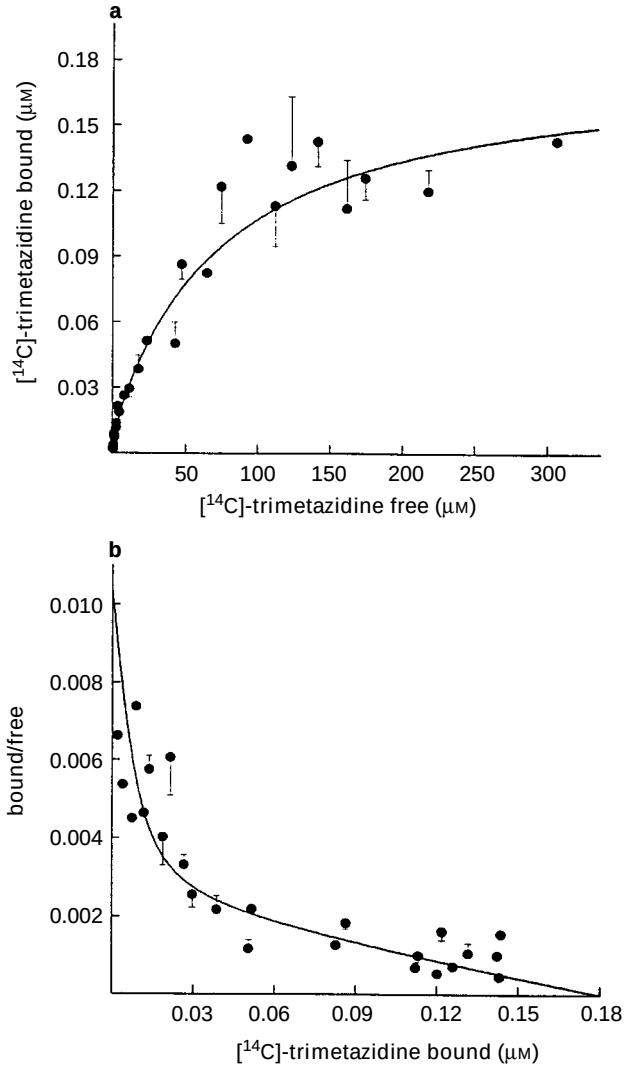

Figure 5 Equilibrium binding of [14C]-trimetazidine to rat liver mitochondria. [14C]-trimetazidine (0.5–300 μM) was incubated with mitochondria (2 mg ml^{-1}) for 45 min at 25°C. Non-specific binding was determined in presence of 50 mM S-00226 and varied from 16% (0.5 μM) to 40% (306 μM). In the same range specific binding varied from 185 d.p.m. to 6971 d.p.m. Values are means for five independent experiments performed in duplicate. Equilibrium binding parameters were estimated by a non-linear regression analysis. (a) Direct plot; (b) Scatchard plot.

binding sites on liver mitochondria (Figure 5). A non-linear regression of the data indicated that high-affinity sites represent only 4% of the total sites ($B_{max_H} = 5$ pmol mg^{-1} protein) with a K_{d_H} value of 0.96 μM. Such a low concentration made the observation difficult when a direct plot was used but a linear Scatchard plot clearly showed their presence. Low-affinity binding sites were much more abundant ($B_{max_L} = 108$ pmol mg^{-1} protein), with a K_{d_L} value of 84 μM. The same binding parameters were found when mitochondria were subjected to hypo-osmotic shock and sonication. This procedure eliminated the possibility of a trimetazidine uptake mechanism which might accumulate the drug within the mitochondria without binding.

Attempts to identify [^{3}H]-trimetazidine binding sites

[^{3}H]-trimetazidine displacement experiments with drugs belonging to various pharmacological classes were performed to characterize the liver mitochondrial binding sites. Potential inhibitors were selected for their known ability to modify transporter activities and ionic fluxes across the mitochondrial membranes and/or to interact with known mitochondrial sites (McEnery & Hoffman, 1994).

As the trimetazidine low-affinity sites were in large excess over the high-affinity sites, a low [^{3}H]-trimetazidine concentration (8 nM) well below its K_d value was used. Under these conditions the observed IC_{50} values are close to the K_i values (Swillens *et al*., 1995) and we observed that [^{3}H]-trimetazidine labelled both families of sites to a comparable extent. This is illustrated in Figure 6, where S-00226, which has higher affinity and better site selectivity than the parent drug, clearly revealed the similar proportion of high ($IC_{50H} = 0.56$ μM) and low-affinity ($IC_{50L} = 142$ μM) sites labelled by [^{3}H]-trimetazidine.

Among the compounds able to displace [^{3}H]-trimetazidine, two groups can be distinguished (Table 2). Biphasic curves were observed with the first group of drugs. Data analysis according to a non-competitive inhibition model ($n_H < 1$) indicated that these drugs recognized two populations of binding sites of high and low-affinity, in good agreement with kinetic and equilibrium experiments. In this group trifluoperazine, dibucaine and prenylamine, which share the common property of inhibiting phospholipase A_2 (Broekemeier *et al*., 1985), were strong inhibitors of [^{3}H]-trimetazidine binding with IC_{50H} values lower than 1 μM, whereas diltiazem and clonazepam, which inhibit the activity of the mitochondrial Na^+-Ca^{2+} exchanger (Cox & Matlib, 1993), were less effective (Table 2).

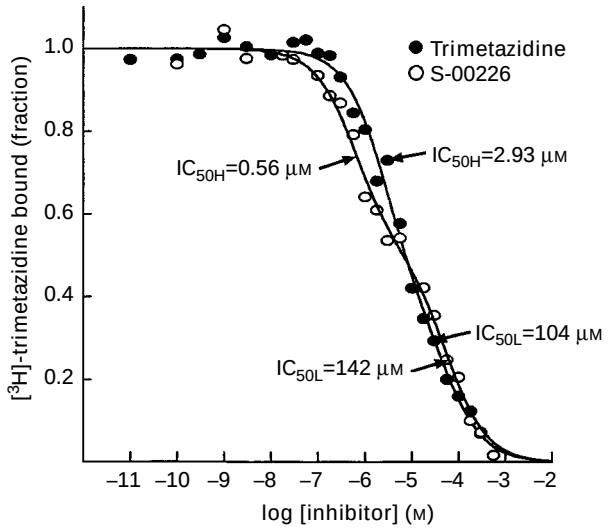

Figure 6 Inhibition of [^{3}H]-trimetazidine binding to rat liver mitochondria (2 mg ml^{-1}) by increasing concentrations of trimetazidine and S-00226. Data are plotted as fractions of the control [^{3}H]-trimetazidine binding value (in the absence of inhibitor: [^{3}H]-trimetazidine bound = 1). [^{3}H]-trimetazidine concentration was 8 nM. Control binding values varied between 16 to 21.5 fmol mg^{-1} protein and non-specific binding between 28 to 35%. Example of data obtained for trimetazidine binding curve: total binding, 3730 d.p.m.; non-specific binding, 1167 d.p.m.

Idazoxan, a marker of the imidazoline-guanidinium-receptive sites (IGRS; Tesson *et al*., 1991), also inhibited [^{3}H]-trimetazidine binding at a low concentration (IC_{50H} = 80 nM; Table 2). However this concentration is ten times higher than the concentration necessary to label IGRS (5 nM; Tesson *et al*., 1991) and trimetazidine affinity for IGRS was very low ($IC_{50} = 338$ μM). These data clearly indicate that the two sites are not identical but suggest that idazoxan is also able to label an additional site different from IGRS on mitochondrial membranes.

The second class of drugs competitively inhibited [^{3}H]-trimetazidine binding with pseudo-Hill coefficients close to 1. As all the molecules tested inhibited 100% of [^{3}H]-trimetazidine binding, we concluded that these drugs bind to the two populations of sites with the same affinity. The most potent drug was nicardipine. It inhibited [^{3}H]-trimetazidine binding with IC_{50} values in the same range as the dissociation constant of [^{3}H]-trimetazidine for the high-affinity sites (≈ 1 μM). This drug is known to interact with the inner membrane anion channel (IMAC; Zernig *et al*., 1990; Beavis, 1989). Propranolol, an inhibitor of anion transport via IMAC (Beavis, 1989), also inhibited [^{3}H]-trimetazidine binding. This suggested a possible relationship between IMAC and trimetazidine sites. We therefore examined the effect of trimetazidine on [^{3}H]-nitrendipine binding, a marker for IMAC (Zernig *et al*., 1990), but no effect was found up to a concentration of trimetazidine of 1 mM. It can therefore be concluded that these sites are not identical.

Diazepam and flunitrazepam which label the voltage-dependent anion channel (VDAC; McEnery, 1992) were also able to displace [^{3}H]-trimetazidine but their affinities were low and protoporphyrin IX, a proposed endogenous ligand of this channel (Verma & Snyder, 1988), was without effect (Table 2). In addition trimetazidine did not inhibit the mitochondrial binding of [^{3}H]-flunitrazepam and [^{3}H]-PK-11195, two markers of the VDAC (data not shown). These data suggest that VDACs are not involved in trimetazidine binding.

Drugs which bind to other mitochondrial targets, including respiratory chain complex inhibitors, adenine nucleotide carrier ligand, a monoamine oxidase (MAO) inhibitor (coumarin) or a Ca^{2+} uniporter blocker (ruthenium red), were ineffective in displacing [^{3}H]-trimetazidine (Table 2). Carnitine, dicyclocarbodiimide, HEPES, inositol 1,4,5-tris-phosphate (IP_3), menadione and oxazepam were also ineffective.

Mitochondrial membrane location of [^{3}H]-trimetazidine binding sites

When mitochondria were subjected to digitonin solubilization with increasing digitonin/protein ratios, [^{3}H]-trimetazidine binding decreased (Figure 7). The release of some of the [^{3}H]-trimetazidine binding sites occurred at low digitonin concentrations which are able to induce the extraction of MAO (an outer membrane marker) without any effect either on cytochrome C oxidase or succinate dehydrogenase activities

Table 2 Inhibition constants of various drugs for [^{3}H]-trimetazidine binding to rat liver mitochondria

Major mitochondrial target	*Compounds*	*Hill model* IC_{50} (μM)	n_H	*Competitive model* IC_{50H} (μM)	IC_{50L} (μM)
Unknown	Trimetazidine	10.9±1.32	0.67±0.03	2.93±0.41	104±22.5
	S-00226	5.22±0.47	0.49±0.03	0.56±0.12	142±17.3
IMAC	Nicardipine	3.90±0.30	1.06±0.25	–	–
	Propranolol	2.90±0.90	0.65±0.01	1.11±0.29	48.2±3.45
	Nitrendipine	109±28	0.99±0.05	–	
Na^+/Ca^{2+} carrier	Diltiazem	74.4±27.9	0.63±0.01	4.57±1.05	232±44.7
	Clonazepam	743±220	0.43±0.06	4.55±1.25	1534±413
VDAC	Diazepam	114±16.5	1.18±0.03	–	–
	Flunitrazepam	237±43.1	0.97±0.04	–	–
	PK-11195	193±30.2	0.70±0.20	–	–
	Protoporphyrin IX		>500		
ANC	ADP		>500		
	ATP		>500		
	Atractyloside		>500		
Ca^{2+} uniporter	Ruthenium red		>500		
K^+/H^+ carrier	Quinine	180±50.8	1.30±0.05	–	–
IGRS	Idazoxan	9.03±1.77	0.46±0.04	0.08±0.02	52.6±16.6
PLA_2	Prenylamine	2.10±0.30	0.52±0.05	0.21±0.05	19.3±3.60
	Trifluoperazine	2.85±0.35	0.47±0.04	0.32±0.08	47.7±8.90
	Dibucaine	9.28±3.06	0.53±0.04	0.86±0.54	93.9±10.1
Cyclophilin	Cyclosporin A		>500		
Chain respiratory complexes	Antimycin		>500		
	Dimethoxy-benzoquinone		>500		
	Rotenone		>500		
Others	Flunarizine	84.0±2.90	0.55±0.04	0.35±0.16	38.7±11.9

Data shown are the mean±s.e. of 3–4 experiments done in duplicate. [^{3}H]-trimetrazidine concentration was 6–8 nM. IC_{50} values were estimated by a non-linear regression analysis either by a Hill or a competitive model where two classes of binding sites were considered when the pseudo-Hill coefficient (n_H) was lower than 1. ANC: adenine nucleotide carrier. PLA_2: phospholipase A_2. –: $IC_{50}=IC_{50H}=IC_{50L}$.

(two inner membrane markers). At 0.6 mg digitonin mg^{-1} protein MAO activity was totally suppressed and 50% of [^{3}H]-trimetazidine binding was eliminated. This binding was found in the digitonin extract enriched in outer membranes and it was characterized by S-00226 inhibition studies (Figure 8). Experimental conditions were identical to those described in Figure 6. The inhibition binding curve was monophasic and the IC_{50} value of S-00226, $IC_{50}=2.20$ μM, clearly demonstrates that these sites correspond to the high affinity sites previously described in intact mitochondria ($IC_{50H}=0.56$ μM, Figure 6 and Table 2). The small decrease in affinity may be accounted for by the detergent. A fraction of the high affinity class of sites also remained in the resulting pellet, i.e. in the inner membrane fraction ($IC_{50H}=0.46$ μM) but it only represented 20% of the binding (Figure 8). This suggests that either high affinity sites are also present in the inner membrane or/and that the digitonin concentration employed (0.6 mg digitonin mg^{-1} protein) did not totally extract the outer membrane. In order to check these results we performed [^{3}H]-trimetazidine binding experiments on inner and outer liver mitochondrial membranes purified according to Graham (1993a). The low recovery in mitochondrial membranes did not allow us to generate binding curves, but we measured binding at a fixed concentration of [^{3}H]-trimetazidine (8 nM). [^{3}H]-trimetazidine binding was detected in the two fractions and was more concentrated in the outer (54.8 fmol mg^{-1} protein) than in the inner membranes (7.9 fmol mg^{-1} protein), which correlates well with the localization of high affinity sites in the outer membranes. Taken together these findings indicate that [^{3}H]-trimetazidine binding sites are located both on the inner and outer membranes of the mitochondria.

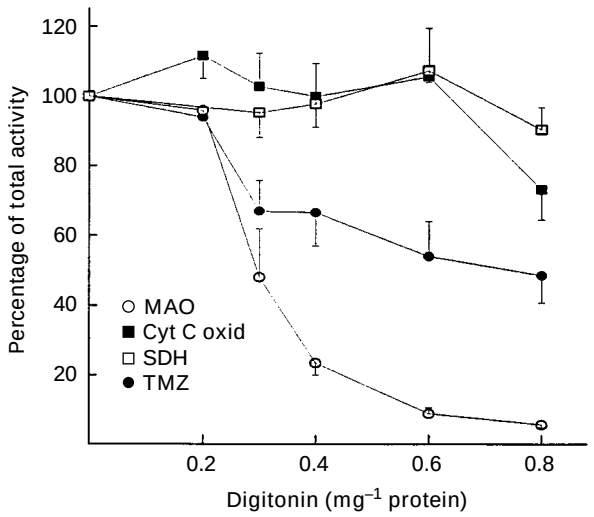

Figure 7 Release of marker enzymes and [^{3}H]-trimetazidine binding sites from isolated hepatocyte mitochondria after digitonin treatment. Freshly isolated mitochondria (M_{H_3} fraction: 8 mg ml^{-1}) were treated with increasing concentrations of digitonin in 1 ml buffer B for 15 min at 4°C. After incubation the mitochondrial suspension was diluted in buffer B and centrifuged at 15,000 *g* for 7 min. Enzymatic activities (MAO, cytochrome C oxidase (Cyt C oxid), succinate dehydrogenase (SDH)) and [^{3}H]-trimetazidine (TMZ; 8 nM) binding were then assayed in the pellet. The maximal activities of the markers (100% values) were 1.51 nM min^{-1} mg^{-1} protein for MAO, 4.80 nmol min^{-1} mg^{-1} protein for cytochrome C oxidase, 2.18 DO min^{-1} mg^{-1} protein for succinate dehydrogenase and 14.75 fmol mg^{-1} protein for [^{3}H]-trimetazidine binding. Each data point is the mean of duplicate measurements obtained from four to five experiments; vertical lines show s.e.mean.

Inhibition of mitochondrial swelling and ability to displace bound [3H]-trimetazidine

We have recently demonstrated (Elimadi *et al*., 1997) that trimetazidine is able to inhibit the mitochondrial swelling induced by *t*-BH plus Ca^{2+}. This effect was dose-dependent ($IC_{50}=200$ μM), mitochondrial swelling being totally inhibited by a trimetazidine concentration of 700 μM. Thus, the last phase of this study was to investigate the possible involvement of [3H]-trimetazidine binding sites in MTP inhibition. This was done by comparing the swelling inhibition and [3H]-trimetazidine displacement capacities of various compounds. These drugs share the common property of being amphiphilic cations acting on various types of membranes where they are considered as ion exchange inhibitors.

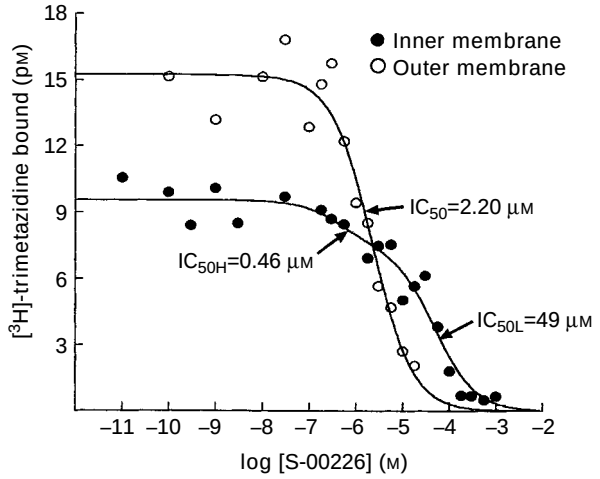

Figure 8 Characterization of [3H]-trimetazidine binding sites in the outer and inner membrane fraction. The binding of [3H]-trimetazidine (8 nM) was measured in the presence of various concentrations of S-00226 in the digitonin preparation enriched in outer membranes (0.62 mg ml^{-1}; specific binding = 1123 d.p.m.) and in the inner membrane fraction (2 mg ml^{-1}; specific binding = 705 d.p.m.).

Most of the drugs that inhibited [3H]-trimetazidine binding also inhibited mitochondrial swelling. Propafenone, prenylamine, flunarizine and trifluoperazine showed a potent effect with IC_{50} values ranging from 13 to 25 μM, whereas acebutolol and prilocaine were the least effective (Table 3). Among the trimetazidine derivatives S-00240 was the most potent ($IC_{50}=23$ μM). Based on these results, a possible relationship between IC_{50} values in binding and swelling experiments was investigated. A correlation between these two parameters could be detected when mean binding IC_{50} values (Hill model, IC_{50} values in Table 3) were used ($r=0.62$; $P<0.01$) but a better correlation was found when low-affinity binding IC_{50L} values (competitive model in Table 3) were considered (Equation 1; $r=0.907$; $P<0.001$). This relationship is presented graphically in Figure 9.

$$pIC_{50}\text{swelling} = 1.016\ pIC_{50L}\text{binding} \qquad (8)$$

In contrast, a poor correlation ($r=0.42$; $P<0.05$) was observed between swelling inhibition and high-affinity [3H]-trimetazidine binding sites (IC_{50H} values in Table 3). It should be noted that results obtained from swelling and binding experiments were comparable, since we verified that the experimental conditions used to study swelling inhibition, i.e. Ca^{2+} plus *t*-BH, did not modify [3H]-trimetazidine binding parameters.

Discussion

This study demonstrated the existence of specific binding sites for the anti-ischaemic agent trimetazidine on isolated rat liver mitochondria. Subcellular distribution indicated that [3H]-trimetazidine binding was mainly associated with mitochondrial fractions but was also present in other cellular fractions. Indeed, [3H]-trimetazidine binding was observed in the

Table 3 Inhibition of mitochondrial swelling and [3H]-trimetazidine binding

Compounds	*IC50*	*IC50 binding* (µM) *IC50H*	*IC50L*	*IC50 swelling* (µM)
1 Trimetazidine	10.9	2.93	104	200
2 S-00226	5.22	0.56	142	320
3 S-00240	12.4	–	–	23
4 S-17316	25.6	1.65	486	400
5 S-64329	1.53	0.02	34.2	54
6 Acebutolol	103	30.6	647	700
7 Alprenolol	2.65	0.54	33.8	33
8 Bupivacaine	108	–	–	223
9 Chlorpromazine	3.40	0.53	19.5	39
10 Deprenyl	11.4	2.90	158	140
11 Dibucaine	9.28	1.22	86.6	50
12 Flunarizine	8.40	0.35	38.7	20
13 Flupentixol	4.93	0.63	56.1	33
14 Prenylamine	2.10	0.21	19.3	15
15 Prilocaine	35.5	10.3	784	900
16 Promethazine	6.40	0.64	22.6	49
17 Propafenone	4.55	–	–	13
18 (+)-Propranolol	2.13	0.52	16.3	33
19 (−)-Propranolol	2.90	1.11	48.2	52
20 Quinacrine	8.00	2.50	106	72
21 Quinidine	36	–	–	45
22 Quinine	180	–	–	130
23 Trifluoperazine	2.85	0.32	47.7	25
24 Verapamil	6.55	1.55	95.4	182

Binding and swelling data are the mean of 3–4 and 3 experiments, respectively. [3H]-trimetazidine concentration was 6–8 nM. IC_{50} values were estimated as described in Table 2. The numbers (1–24) refer to Figure 9. To enhance clarity, s.e. values were not included in the table. –: $IC_{50}=IC_{50H}=IC_{50L}$.

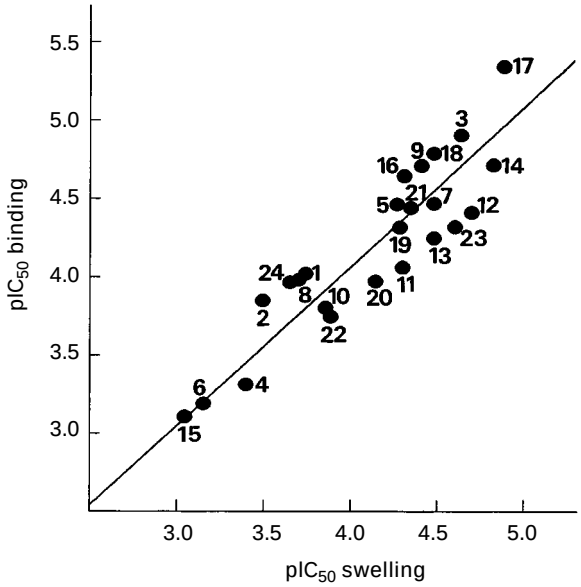

Figure 9 Relationship between the affinity of drugs for the mitochondrial [^{3}H]-trimetazidine binding sites and their potency in the swelling inhibition experiments. Plotted are pIC_{50} values for inhibition of mitochondrial swelling versus pIC_{50L} values (listed in Table 3) for the low-affinity mitochondrial [^{3}H]-trimetazidine binding. For key to the numbers (1–24) refer to Table 3. The regression line was obtained by least squares fit analysis of the data points.

microsomal fraction although it was devoid of cytochrome C oxidase activity and, thus, of mitochondria. These microsomal sites correspond probably to sites of biotransformations as trimetazidine is metabolized in man and in rats, probably in the liver (Harpey *et al*., 1989; Jackson *et al*., 1996). The large binding recovery in the nuclear fraction can be attributed to the presence of mitochondria, as assessed by cytochrome C oxidase activity remaining in this fraction.

Two classes of specific binding sites of high and low affinity were observed on mitochondria. The high affinity component ($K_d = 1$ μM) represented 4% of the total sites. It was located on the outer membrane, whereas the low affinity seemed to be restricted to the mitochondrial inner membrane.

Displacement experiments showed some degree of interaction between [^{3}H]-trimetazidine binding sites and some identified mitochondrial binding markers of VDAC, IMAC, Na^+/Ca^{2+} exchanger and IGRS. However, the criteria of a competitive inhibition were not fulfilled as even if [^{3}H]-trimetazidine was displaced by these drugs, the reverse was not observed. Thus [^{3}H]-trimetazidine binding sites are distinct from these mitochondrial targets. Nevertheless, it was interesting to note that flunarizine which promotes Ca^{2+} efflux from Ca^{2+}-loaded mitochondria (Uceda *et al*., 1995), like trimetazidine (Salducci *et al*., 1996), also inhibited [^{3}H]-trimetazidine binding. This Ca^{2+} extrusion mechanism is unknown but is apparently independent of Na^+ (Uceda *et al*., 1995) and could be a common target for trimetazidine and flunarizine. Diltiazem and clonazepam were also effective inhibitors of [^{3}H]-trimetazidine binding. These drugs have been found to inhibit the activity of the mitochondrial Na^+-Ca^{2+} exchanger (Cox & Matlib, 1993) within the same concentration range (7 μM) as that which displaces [^{3}H]-trimetazidine from its high-affinity binding sites (4–5 μM). However, as the Na^+-Ca^{2+} carrier is poorly concentrated in liver mitochondria (Gunter & Pfeiffer, 1990), such a mechanism does not seem relevant. Another possible target of trimetazidine action might be phospholipases. Indeed trifluoperazine, dibucaine and prenylamine, which share the common property of inhibiting phospholipase A_2 (Broekemeier *et al*., 1985), were strong inhibitors of [^{3}H]-trimetazidine binding with IC_{50} values for its high-affinity sites lower than 1 μM (Table 2). These data may be related to the fact that phospholipase A_2 inhibitors were shown to inhibit mitochondrial swelling and, thus, to protect mitochondria against the damage induced by the association of a prooxidant and Ca^{2+} (Broekemeier *et al*., 1985; Pereira *et al*., 1992). This property is shared by trimetazidine which is able to inhibit mitochondrial swelling under the same conditions. However, a possible modulation of phospholipase A_2 activity by trimetazidine remains to be established.

The relationship between the inhibitory potency of various compounds towards mitochondrial swelling induced by the activation of the MTP, and their affinity for [^{3}H]-trimetazidine binding sites indicates that the two structures could be associated. It also suggests that trimetazidine inhibits MTP by interacting with its low-affinity binding sites. These sites are not yet identified. A likely explanation would be that trimetazidine interacts with the MTP inhibitory sites already described for divalent cations (Bernardi *et al*., 1993). The fact that such sites have been found on the cytoplasmic side of mitochondrial membrane, but that the same or other inhibitory sites are accessible from the matrix side (Zoratti & Szabo', 1995) is in accordance with the localization of trimetazidine binding sites on both the outer and inner mitochondrial membranes. However, further experiments are needed to clarify the localization of the trimetazidine low-affinity binding sites.

A change in the mitochondrial surface potential has also been proposed to explain the closure of the pore (Broekemeier & Pfeiffer, 1995). Indeed cationic compounds such as sphingosine (Broekemeier & Pfeiffer, 1995), trifluoperazine (Pereira *et al*., 1992), spermine (Lapidus & Sokolove, 1994) and divalent cations (Bernardi *et al*., 1993), which are believed to render the membrane potential more positive, inhibit pore opening. This hypothesis may be applied to trimetazidine which is a divalent cation and could perhaps modify the surface potential.

It has been observed that some drugs known to inhibit MTP do not displace [^{3}H]-trimetazidine. This is especially the case for cyclosporin A. Halestrap & Davidson (1990) have proposed a model to explain the effect of cyclosporin A. They suggest that the combination of cyclosporin A with a matrix enzyme, cyclophilin, prevents the opening process. Some of us have recently observed that trimetazidine acts by a quite independent mechanism (Elimadi *et al*., 1997). This finding emphasizes the fact that the MTP regulation involves several independent mechanisms, even when the same inducing process is involved (see Zoratti & Szabo', 1995).

In conclusion, the present results demonstrate the existence of two families of [^{3}H]-trimetazidine binding sites located both on the outer and the inner mitochondrial membranes. These sites are distinct from all mitochondrial sites described to date. Our results suggest that they may be implicated in the closure of the mitochondrial permeability transition pore.

We thank Dr A. Le Ridant, Institut de Recherches Internationales Servier, for his help and his gift of unlabelled and labelled trimetazidine and analogues. We also gratefully acknowledge Dr R. Andrade (Department of Psychiatry, Wayne State University of Detroit) for rereading the manuscript. This work was supported by the Institut de Recherches Internationales Servier, the Ministère de l'Education Nationale (DRED EA 427), and the Réseau de Pharmacologie Clinique.

References

ANHOLT, R.R., PEDERSEN, P.L., DE SOUZA, E.B. & SNYDER, S.H. (1986). The peripheral-type benzodiazepine receptor. Localization to the mitochondrial outer membrane. *J. Biol. Chem.,* **261,** 576–583.

BEAVIS, A.D. (1989). On the inhibition of the mitochondrial inner membrane anion uniporter by cationic amphiphiles and other drugs. *J. Biol. Chem.,* **264,** 1508–1515.

BEMBENEK, M.E., ABELL, C.W., CHRISEY, L.A., ROZWADOWSKA, M.D., GESSNER, W. & BROSSI, A. (1990). Inhibition of monoamine oxidases A and B by simple isoquinoline alkaloids: racemic and optically active 1,2,3,4-tetrahydro, 3-4-dihydro and fully aromatic isoquinolines. *J. Med. Chem.,* **33,** 147–152.

BERNARDI, P., VERONESE, P. & PETRONILLI, V. (1993). Modulation of the mitochondrial cyclosporin A-sensitive permeability transition pore. *J. Biol. Chem.,* **268,** 1005–1010.

BROEKEMEIER, K.M. & PFEIFFER, D.R. (1995). Inhibition of the mitochondrial permeability transition by cyclosporin A during long time frame experiments: relationship between pore opening and the activity of mitochondrial phospholipases. *Biochemistry,* **34,** 16440–16449.

BROEKEMEIER, K.M., SCHMID, P.C., SCHMID, H.A.O. & PFEIFFER, D.R. (1985). Effects of phospholipase A_2 inhibitors on ruthenium red-induced Ca^{2+} release from mitochondria. *J. Biol. Chem.,* **260,** 105–113.

COX, D.A. & MATLIB, M.A. (1993). Modulation of intramitochondrial free Ca^{2+} by antagonists of Na^{+}-Ca^{2+} exchanger. *Trends Pharmacol. Sci.,* **14,** 408–413.

ELIMADI, A., MORIN, D., SAPENA, R., CHAUVET-MONGES, A.M., CREVAT, A. & TILLEMENT, J.P. (1997). Comparison of the effects of cyclosporine A and trimetazidine on Ca^{2+}-dependent mitochondrial swelling. *Fundam. Clin. Pharmacol.,* **11,** 440–447.

GRAHAM, J.M. (1993a). Methods in molecular biology. In *Biomembrane Protocols*. ed. Graham, J.M. & Higgins, J.A. pp. 29–40. Totowa, New Jersey: Humana Press.

GRAHAM, J.M. (1993b). Methods in molecular biology. In *Biomembrane Protocols*. ed. Graham, J.M. & Higgins, J.A. pp. 1–18. Totowa, New Jersey: Humana Press.

GUARNIERI, C. & MUSCARI, C. (1993). Effect of trimetazidine on mitochondrial functions and oxidative damage during reperfusion of ischemic hypertrophied rat myocardium. *Pharmacology,* **46,** 324–331.

GUNTER, T.E. & PFEIFFER, D.R. (1990). Mechanisms by which mitochondria transport calcium. *Am. J. Physiol.,* **258** (*Cell Physiol.,* **27**), C755–C786.

HALESTRAP, A.P. & DAVIDSON, A.M. (1990). Inhibition of Ca^{2+}-induced large-amplitude swelling of liver and heart mitochondria by cyclosporin A is probably caused by the inhibitor binding to mitochondrial-matrix peptidyl-prolyl *cis-trans* isomerase and preventing it from interacting with the adenine nucleotide translocase. *Biochem. J.,* **268,** 153–160.

HARPEY, C., CLAUSER, P., LABRID, C., FREYRIA, J.L. & POIRIER, J.P. (1989). Trimetazidine, a cellular anti-ischemic agent. *Cardiovasc. Drug Rev.,* **6,** 292–312.

HAWORTH, R.A. & HUNTER, D.R. (1979). The Ca^{2+}-induced membrane transition in mitochondria. II Nature of the Ca^{2+} trigger site. *Arch. Biochem. Biophys.,* **195,** 460–467.

JACKSON, P.J., BROWNSILL, R.D., TAYLOR, A.R., RESPLANDY, G., WALTHER, B. & SCHWIETERT, H.R. (1996). Identification of trimetazidine metabolites in human urine and plasma. *Xenobiotica,* **26,** 221–228.

JOHNSON, D. & LARDY, H.A. (1967). Isolation of liver and kidney mitochondria. In *Methods in Enzymology* ed. Estabook, R.W. & Pullman, M. Vol 10, pp. 94–96. New York: Academic Press.

KOENIG, H. (1974). The isolation of lysosomes from brain. In *Methods in Enzymology* ed. Fleischer, S. & Packer, L. Vol 31, pp. 457–477. New York: Academic Press.

LAPIDUS, R.G. & SOKOLOVE, P.M. (1994). The mitochondrial permeability transition. Interactions of spermine, ADP, and inorganic phosphate. *J. Biol. Chem.,* **269,** 18931–18936.

LAVANCHY, N., MARTIN, J. & ROSSI, A. (1987). Antiischemic effect of trimetazidine: P-31 NMR spectroscopy in the isolated rat heart. *Arch. Int. Pharmacodyn. Ther.,* **286,** 97–110.

LEFUR, G., VAUCHER, N., PERRIER, M.L., FLAMIER, A., BENAVIDES, J., RENAULT, C., DUBROEUCQ, M.C., GUEMERY, C. & UZAN, A. (1983). Differentiation between two ligands for peripheral benzodiazepine binding sites, [^{3}H]-RO5-4864 and [^{3}H]-PK-11195, by thermodynamic studies. *Life Sci.,* **33,** 449–457.

LOWRY, O.H., ROSEBROUGH, N.J., FARR, A.L. & RANDALL, R.J. (1951). Protein measurement with the folin phenol reagent. *J. Biol. Chem.,* **93,** 265–275.

MCENERY, M.W. (1992). The mitochondrial benzodiazepine receptor: evidence for association with the voltage-dependent anion channel (VDAC). *J. Bioenerg. Biomembr.,* **24,** 63–69.

MCENERY, M.W. & HOFFMAN, R.D. (1994). The use of ligand binding technics to identify transport proteins: the characterisation of the [^{125}I]-iodophenylarsine oxide receptor in rat mitochondrial membranes. In *Molecular Biology of Mitochondrial Transport Systems*. ed. Forte, M. & Colombini, M. NATO ASI Series, H 83, pp. 99–116. Berlin: Springer-Verlag.

MORIN, D., ZINI, R., URIEN, S., SAPENA, R. & TILLEMENT, J.P. (1992). Labelling of rat brain β-adrenoceptors: (^{3}H)CGP-12177 or (^{125}I)iodocyanopindolol? *J. Receptor Res.,* **12,** 369–387.

PEREIRA, R.S., BERTOCCHI, A.P.F. & VERCESI, A.E. (1992). Protective effect of trifluoperazine on the mitochondrial damage induced by Ca^{++} plus prooxydants. *Biochem. Pharmacol.,* **44,** 1795–1801.

RUSTIN, P., CHRETIEN, D., BOURGERON, T., GERARD, B., ROTIG, A., SAUDUBRAY, J.M. & MUNNICH, A. (1994). Biochemical and molecular investigations in respiratory chain deficiencies. *Clin. Chim. Acta,* **228,** 35–51.

SALDUCCI, D., CHAUVET-MONGES, A.M., TILLEMENT, J.P., ALBENGRES, E., TESTA, B., CARRUPT, P. & CREVAT, A. (1996). Trimetazidine reverses calcium accumulation and impairment of phosphorylation induced by cyclosporine A in isolated rat liver mitochondria. *J. Pharmacol. Exp. Ther.,* **277,** 417–422.

SWILLENS, S., WAELBROECK, M. & CHAMPEIL, P. (1995). Does a radioligand bind to a homogeneous population of non-interacting receptor sites? *Trends Pharmacol. Sci.,* **16,** 151–155.

TESSON, F., PRIP-BUUS, C., LEMOINE, A., PEGORIER, J.P. & PARINI, A. (1991). Subcellular distribution of imidazoline-guanidinium-receptive sites in human and rabbit liver. *J. Biol. Chem.,* **266,** 155–160.

UCEDA, G., GARCIA, A.G., GUANTES, J.M., MICHELENA, P. & MONTIEL, C. (1995). Effects of calcium channel antagonists on mitochondrial Ca^{2+} transport. *Eur. J. Pharmacol.,* **289,** 73–80.

URIEN, S. (1995). Micropharm-K, a microcomputer interactive program for the analysis and simulation of pharmacokinetic processes. *Pharmacol. Res.,* **12,** 1225–1230.

VERMA, A. & SNYDER, S.H. (1988). Characterization of porphyrin interaction with peripheral-type benzodiazepin receptors. *Mol. Pharmacol.,* **34,** 800–805.

WEILAND, G.A. & MOLINOFF, P.B. (1981). Minireview: quantitative analysis of drug-receptor interactions: I determination of kinetic and equilibrium properties. *Life Sci.,* **29,** 313–330.

ZERNIG, G., GRAZIADEI, I., MOSHAMMER, T., ZECH, C., REIDER, N. & GLOSSMAN, H. (1990). Mitochondrial Ca^{2+} antagonists binding sites are associated with an inner mitochondrial membrane anion channel. *Mol. Pharmacol.,* **38,** 362–369.

ZORATTI, M. & SZABO', I. (1995). The mitochondrial permeability transition. *Biochim. Biophys. Acta,* **1241,** 139–176.

(Received July 10, 1997
Revised December 23, 1997
Accepted January 6, 1998)